

Cu(II), Ni(II), Zn(II) and Fe(III) complexes containing a N₂O₂ donor ligand: Synthesis, characterization, DNA cleavage studies and crystal structure of [Cu(HL)Cl]

Rakesh S. Sancheti^a, Ratnamala S. Bendre^{a,*}, Anupa A. Kumbhar^b

^a School of Chemical Sciences, North Maharashtra University, Jalgaon 425001, India

^b Department of Chemistry, University of Pune, Pune 411007, India

ARTICLE INFO

Article history:

Received 29 April 2011

Accepted 21 June 2011

Available online 23 July 2011

Keywords:

Polydentate ligand

Crystal structure

Oxidative DNA cleavage

DNA binding

Cu(II)

ABSTRACT

A polydentate ligand, **H₂L** “[1-(5-isopropyl-2-methyl phenoxy)-3-(N-2-hydroxy benzyl-N-((pyridine-2-yl)amino) propan-2-ol)]”, containing a N₂O₂ donor moiety was synthesized by refluxing 2-((5-isopropyl-2-methylphenoxy)methyl)oxirane and HBPA (N-(2-hydroxybenzyl)-N-(2-pyridylmethyl)amine). This synthesized ligand was used for the preparation of complexes with different metal ions, viz. [Cu(HL)Cl] (**1**), [Ni(HL)Cl] (**2**), [Zn(HL)Cl] (**3**) and [Fe(HL)Cl₂] (**4**). The ligand and metal complexes were characterized by ¹H NMR, mass, ESI-MS, elemental analysis, IR, UV-Vis and electron paramagnetic resonance (EPR) spectroscopy. The crystal structure for one of the complexes, [Cu(HL)Cl], was solved from the X-ray crystallography data. The structure of the complex, based on the trigonality index tau, suggests an intermediate geometry between square pyramidal (sp) and trigonal bipyramidal (tb). Both the ligand and the metal complexes show oxidative cleavage of plasmid DNA (pBR322) without addition of any exogenous agent, even at a concentration of 5 μM. The binding constants for these compounds were found to be in the range 5.33–0.065 × 10⁵ M⁻¹.

© 2011 Elsevier Ltd. All rights reserved.

1. Introduction

Earlier, transition metal complexes were thought to be an odd choice for studying DNA interactions, however over the last few years they have become attractive agents for nuclease activity as they possess different structures and reactivities. With few exceptions, biological transition metals are confined to coordination sites in proteins or cofactors, and are not in discrete, freestanding coordination complexes [1,2].

Molecules possessing the ability to bind and cleave double stranded DNA under physiological conditions are explored as diagnostic agents in medicinal applications and for the development of genomic research [3–24]. Generally DNA cleavage follows an oxidative or hydrolytic cleavage pathway. The hydrolytic pathway proceeds through hydrolysis of the phosphodiester bond, leading to fragmentation of DNA, and such pathways are mediated by enzymatic processes, while the oxidative process involves the oxidation of nucleobases and/or H abstraction from the sugar moiety [25].

Metal-based synthetic nucleases are of interests for their varied applications in nucleic acid chemistry, including the design of DNA and RNA specific agents capable of controlled cleavage. They are important because of their potential use as chemotherapeutic

drugs, gene regulators and molecular biological tools [26,27]. Although redox active transition metal complexes in the presence of oxidants have been extensively used for DNA cleavage reactions, the complexes [Fe(EDTA)]²⁻ [28] (EDTA = ethylene diaminetetraacetic acid), [Cu(phen)₂]⁺ [29] (phen = 1,10-phenanthroline), [Fe-BLM] [30] (BLM = bleomycin), metalloporphyrins [31], Ni-azamacrocycles [32], [Mn(salen)]³⁺ [33] (salen = N,N'-ethylenebis(salicylaldeneaminato), [Cu-desferal] [34], [Co-cyclam] [35], [Rh(phen)₂(phi)]³⁺ and [Rh(en)₂(phi)]³⁺ [36] (en = N,N'-ethylenediamine; phi = 9,10-phenanthrenequinone diimine), possessing diverse structures and nucleotidal reactivity, have also been reported as prospective candidates. However, the initiation of cleavage in most cases requires exogenous agents such as H₂O₂, mercaptopropionic acid, dithiothreitol or light. This fact limits their in vitro applications; hence DNA cleaving agents functioning without any activation are desirable. Lamour et al. [37], Sissi et al. [38] and Tonde et al. [39] have reported polyhydroxy copper based systems that trigger self activating nuclease activity.

Considering the very sensitive nature of DNA towards oxidative cleavage, efforts have been directed towards the development of molecules capable of cleaving DNA with an oxidative mechanism [40]. Numerous efficient cleaving agents such as reactive oxygen species (ROS) or free radicals capable of inducing an oxidative pathway have been developed over the course of time. The antitumor, antibiotic, drug leinamycin and its analogs have exhibited the crucial role of “Chemical Nucleases” through reduction of molecular oxygen to form reactive hydroxyl species [41,42].

* Corresponding author. Fax: +91 0257 2257431.

E-mail address: bendres@rediffmail.com (R.S. Bendre).

Thus, in the present work, we report the DNA cleavage activity of novel asymmetric polydentate ligand and transition metal complexes prepared with this ligand.

2. Materials and methods

All reagents and chemicals were purchased from commercial sources and were used without further purification. N-(2-hydroxybenzyl)-N-(2-pyridylmethyl)amine (HBPA) was synthesized by the reported method [43]. Plasmid DNA (pBR322) and calf thymus (Genei, Bangalore, India), superoxide dismutase (SOD), (Sigma, stored at -20°C), agarose and boric acid (Molecular Biology grade, Sisco Research Laboratories, India), tris(hydroxymethyl)aminomethane (TRIS, AR Grade) and ethylene diaminetetraacetic acid (EDTA, AR Grade, Sisco Research Laboratories, India) were used as received. Ultrapure MilliQ water was used for all the experiments.

3. Experimental

The synthesis of the ligand involves various steps as shown in Scheme 1.

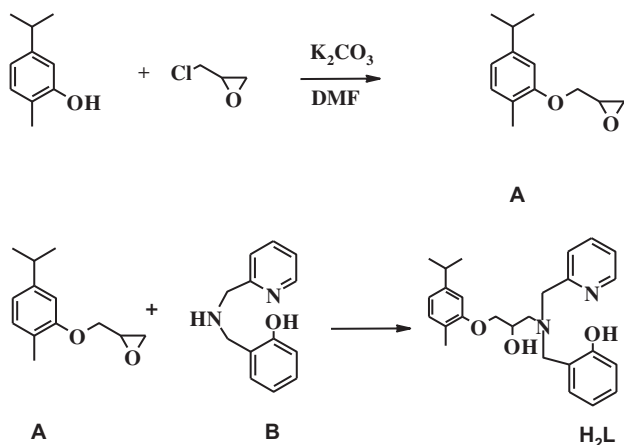
3.1. Synthesis of 2-((5-isopropyl-2-methylphenoxy)methyl)oxirane (A)

2-((5-isopropyl-2-methylphenoxy)methyl)oxirane was synthesized by the reaction of 5-isopropyl-2-methyl phenol (6.6 mmol, 1.00 g) with epichlorohydrin in excess (13.2 mmol, 1.84 g) in the presence of K_2CO_3 (13.3 mmol, 1.83 g) in 20 ml DMF (N,N-dimethylformamide) at 70°C , stirring for 8 h. The resulting product was dissolved in water and extracted with three 20 ml portions of hexane. The combined organic extracts were dried over anhydrous Na_2SO_4 and the solvent was removed under reduced pressure to give a brown oil.

Yield: 80%; B.P.: 120°C ; ^1H NMR (ppm, CDCl_3): 1.23 (d, 6H, 2CH_3), 2.20 (s, 3H, Ar- CH_3), 2.85 (m, 1H, oxirane-CH), 3.38 (m, 1H, Ar-CH), 3.95 (d, 2H, oxirane- CH_2), 4.21 (d, 1H, $-\text{CH}_2$), 6.65 (s, 1H, ArH), 6.8 (d, 1H, ArH), 7.1 (d, 1H, ArH). IR/ cm^{-1} : $\nu(\text{C}-\text{O})$ 1255; $\nu(\text{C}=\text{C})$ 1416, 1511, 1612 (Supplementary Figs. S3 and S6).

3.2. Synthesis of N-(2-hydroxybenzyl)-N-(2-pyridylmethyl)amine (HBPA) (B)

N-(2-hydroxybenzyl)-N-(2-pyridylmethyl)amine (HBPA) was synthesized according to the previously reported procedure [43]:



Scheme 1. Schematic representation of the synthesis of the ligand H_2L .

3.3. Synthesis of 1-(5-isopropyl-2-methyl phenoxy)-3-(N-2-hydroxybenzyl)-N-((pyridine-2-yl)amino)propan-2-ol (H_2L)

This compound was synthesized by reacting compound A (5.8 mmol, 1.20 g) with B (5.8 mmol, 1.23 g) in methanol under reflux at 70°C for 8 h. The reaction mixture was cooled, filtered and the precipitated product was washed with cold methanol to remove the impurities.

Yield: 66%, M.P.: 134°C ; ^1H NMR (ppm, CDCl_3): 1.20 (d, 6H, $2-\text{CH}_3$), 2.08 (s, 3H, $-\text{CH}_3$), 2.84 (d, 2H, $-\text{CH}_2$), 3.10 (m, 1H, $-\text{CH}$), 3.90 (m, 4H, $2-\text{CH}_2$), 4.10 (d, 2H, $-\text{CH}_2$), 4.25 (m, 1H, $-\text{CH}$), 4.58 (bs, 1H, Ar-OH), 6.7–7.7 (Ar-H). Anal. Calc. for $\text{C}_{26}\text{H}_{32}\text{O}_3\text{N}_2$: C, 74.44; H, 7.44; N, 7.05. Found: C, 74.54; H, 7.37; N, 6.67%. IR (cm^{-1}): $\nu(\text{C}=\text{C})$ 1586, $\nu(\text{C}-\text{O}-\text{C})$ 1151. MS (m/z): 421 [M] $^+$ (Supplementary Figs. S3, S1, S6, and S4).

3.4. Synthesis of the complexes

3.4.1. Synthesis of $[\text{Cu}(\text{HL})\text{Cl}]$ (1)

A 10 ml methanolic solution of H_2L (2 mmol, 0.80 g) and a methanolic solution of $\text{CuCl}_2 \cdot 2\text{H}_2\text{O}$ (2 mmol, 0.32 g) were mixed and refluxed for 5–8 h. Triethylamine was added in a catalytic amount for acceleration of the reaction. After cooling the solution to room temperature, a stable green microcrystalline precipitate was formed, which was filtered off and washed with water, ethanol and then ether. Single crystals, suitable for X-ray crystallography, were obtained from methanol/DCM. Yield: 60%; Anal. Calc. for $\text{CuC}_{26}\text{H}_{31}\text{O}_3\text{N}_2\text{Cl}$: C, 60.22; H, 6.02; N, 5.40. Found: C, 58.91; H, 5.92; N, 5.42%. ESI-MS m/z , ion 482.2 [M] $^+$ (Supplementary Figs. S1 and S4).

3.4.2. Synthesis of $[\text{Ni}(\text{HL})\text{Cl}]$ (2), $[\text{Zn}(\text{HL})\text{Cl}]$ (3) and $[\text{Fe}(\text{HL})\text{Cl}_2]$ (4)

Complexes 2, 3 and 4 were prepared by a similar procedure as for complex 1, using $\text{NiCl}_2 \cdot 6\text{H}_2\text{O}$, ZnCl_2 and FeCl_3 instead of $\text{CuCl}_2 \cdot 2\text{H}_2\text{O}$. Complex 2, (light green): yield, 70%; Anal. Calc. for $\text{NiC}_{26}\text{H}_{31}\text{O}_3\text{N}_2\text{Cl}$: C, 60.79; H, 6.07; N, 5.45. Found: C, 60.40; H, 5.99; N, 6.79%. ESI-MS m/z , ion 477.2 [M] $^+$. Complex 3, (white): yield, 62%. Anal. Calc. for $\text{ZnC}_{26}\text{H}_{31}\text{O}_3\text{N}_2\text{Cl}$: C, 60.00; H, 6.00; N, 5.38. Found: C, 58.62; H, 5.94; N, 6.56%. ESI-MS m/z , ion 483.2 [M] $^+$. Complex 4, (blue): yield: 78%. Anal. Calc. for $\text{FeC}_{26}\text{H}_{31}\text{O}_3\text{N}_2\text{Cl}_2$: C, 57.13; H, 5.53; N, 5.12. Found: C, 58.67; H, 6.01; N, 6.73%. ESI-MS m/z , ion 510.2 [M] $^+$ (Supplementary Figs. S1 and S4).

3.5. Physical measurements

Elemental analyses (C, H and N) were recorded on a Thermo-Finnigan elemental analyzer. ^1H NMR spectra were recorded on a Varian-300 spectrometer. All chemical shifts are relative to tetramethylsilane (TMS). UV–Vis spectra were recorded on a Chemito spectrophotometer (Supplementary Fig. S2). The X-band frozen glass EPR spectra of the Cu complex in dimethyl formamide solutions were recorded on a Varian E-109 spectrometer using tetracyanoethylene (TCNE) as a standard.

3.6. X-Ray crystallography

A green crystal of 1 having the size $0.27 \times 0.12 \times 0.09$ mm was obtained by slow evaporation of the reaction mixture and it was mounted on the tip of a glass fiber. Intensity data were collected on a Bruker SMART APEX diffractometer equipped with a CCD area detector using $\text{MoK}\alpha$ ($\lambda = 0.71073 \text{ \AA}$) radiation at 293 K. The data integration and reduction were processed with SAINT [44] software. An empirical absorption correction was applied with SADABS [45]. The structure was solved by direct methods using SHELXS [46] and refined on F^2 by the full-matrix least-squares technique using the

SHELXL-97 [47] program package. Graphics are generated using ORTEP [48], PLATON [49] and MERCURY.

3.7. Crystal data and structure refinement for [Cu(HL)Cl]

$C_{26}H_{31}ClCuN_2O_3$, $M = 518.52$, triclinic cell, space group $P\bar{1}$, $a = 10.3831(12)$, $b = 12.442(14)$, $c = 12.1536(14)$ Å, $\alpha = 64.950(2)^\circ$, $\beta = 75.800(2)^\circ$, $\gamma = 74.498(2)^\circ$, $V = 1322.4$ Å³, $Z = 2$, $D_{\text{calc}} = 1.302$ mg/m³, $\mu(\text{MoK}\alpha) = 0.955$ mm⁻¹, $F(000) = 542$, $T = 293(2)$ K, 4615 independent reflections ($R_{\text{int}} = 0.0263$) with θ range for data collection 1.87–25.000. Refinement converged at final R_1 [for selected data with $I > 2\sigma(I)$] = 0.0650, wR_2 (all data) = 0.0803, GOF = 1.050.

3.8. DNA cleavage experiments

The DNA cleavage was carried out by agarose gel electrophoresis on a 10 µl total sample volume in 0.5 ml transparent Eppendorf microcentrifuge tubes containing pBR322 DNA (300 ng). For the gel-electrophoresis experiments, pBR322 DNA was treated with the ligand and metal complexes (5–20 µM), and the mixture was incubated for 30 min at 37 °C. The samples were analyzed in 1% agarose gel in (Tris–boric acid–EDTA (TBE) buffer, pH 8.2) for 4 h with a current 60 V cm⁻¹. The gel was stained with a 0.5 µg/ml ethidium bromide, visualized by UV light and photographed for analysis. The extent of cleavage of the SC (supercoiled) DNA was determined by measuring the intensities of the bands using the Alpha Innotech gel documentation system (AlphaImager 2200). For mechanistic investigations, experiments were carried out in presence of different radical scavenging agents such as DMSO, D-mannitol, DABCO, NaN₃, L-histidine and SOD to pBR322 DNA prior to the addition of the complex. Samples were incubated for 60 min at 37 °C.

3.9. DNA binding study

The DNA binding study was carried out using a Chemito UV–Vis spectrophotometer using a 1 ml quartz cuvette. The titrations were performed by keeping the concentration of the compounds constant (50 µM), and varying the concentration of CT-DNA from 0 to 50 µM. The purity of CT-DNA was determined from the ratio of A_{260}/A_{280} , which gave a value of 2:1, and it was used as supplied. From the spectroscopic titration, which was monitored at 260 nm,

Table 1
Selected bond lengths (Å) and bond angles (°).

Cu(1)–O(3)	1.937(3)	O(3)–Cu(1)–N(2)	145.03(15)
Cu(1)–N(2)	2.035(4)	O(3)–Cu(1)–N(1)	92.77(15)
Cu(1)–N(1)	2.062(4)	N(2)–Cu(1)–N(1)	80.71(14)
Cu(1)–Cl(1)	2.2393(15)	O(3)–Cu(1)–Cl(1)	93.43(12)
Cu(1)–O(2)	2.247(3)	N(2)–Cu(1)–Cl(1)	95.58(12)
		N(1)–Cu(1)–Cl(1)	173.29(12)
		O(3)–Cu(1)–O(2)	108.07(14)
		N(2)–Cu(1)–O(2)	104.47(14)
		N(1)–Cu(1)–O(2)	79.60(13)
		Cl(1)–Cu(1)–O(2)	96.04(11)

the binding constants (K_b) of the compounds were determined from the half reciprocal of the plot, as reported [50], given by Eq. (1).

$$D/\Delta\epsilon_{\text{ap}} = 1/\Delta\epsilon * D + 1/\Delta\epsilon K \quad (1)$$

where, $\Delta\epsilon_{\text{ap}} = |\epsilon_a - \epsilon_f|$, $\Delta\epsilon = |\epsilon_B - \epsilon_F|$ and ϵ_a , ϵ_f and ϵ_B are the apparent, free and bound ligand extinctions, respectively. D is the DNA binding concentration in base pairs for native DNA and potential base pairs (half the concentration of bases) for denatured DNA. The half reciprocal of the plot [50], which is generally considered more accurate as compared to the double reciprocal plot proposed by Schmechel and Crothers [51]. K is given by the ratio of the slope to y intercept.

4. Results and discussion

4.1. X-ray structure of [Cu(HL)Cl]

As shown in Fig. 1, the crystallographically independent Cu(II) ion is pentacoordinated by two nitrogen atoms (amine N1 and pyridine N2), two oxygen donors (alkoxy O2 and phenoxy O3) and a chloride ion. Although **H₂L** could behave as a pentadentate bidentate ligand, in the present complex it was found to act as a negative tetradentate ligand. The O1 oxygen of the ether linkage does not participate in coordination, while the O2 oxygen of the hydroxyl group (O2–H2 = 0.93 Å) is coordinated without deprotonation. The OH hydrogen atom is involved in hydrogen bonding with O3 (O3–H2 = 2.643 Å) of a neighboring complex molecule. The coordination sphere is of the type CuN₁N₂O₂O₃Cl₁, exhibiting a geometry in between trigonal bipyramidal (tbp) and square pyramidal (sp). The coordination geometry of [Cu(HL)Cl] can best be

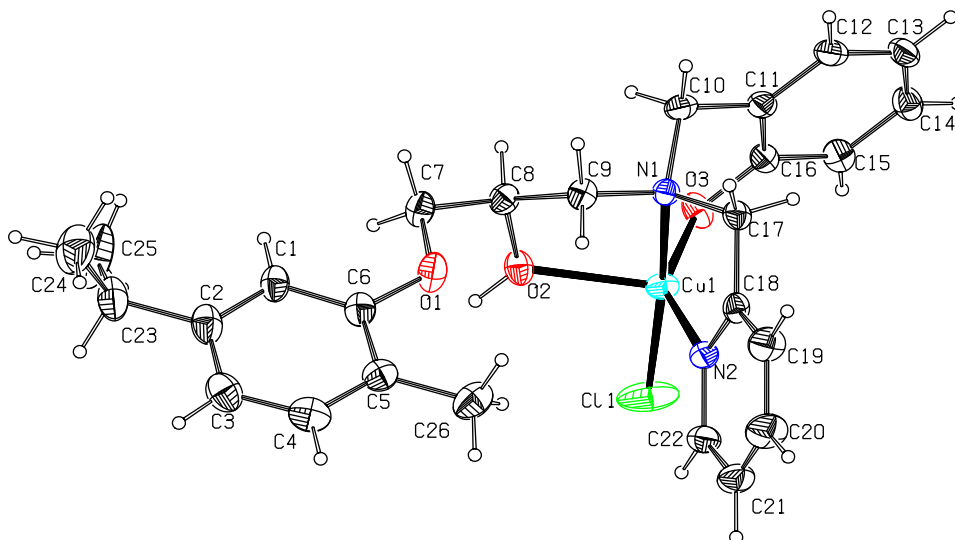


Fig. 1. ORTEP view of [Cu(HL)Cl].

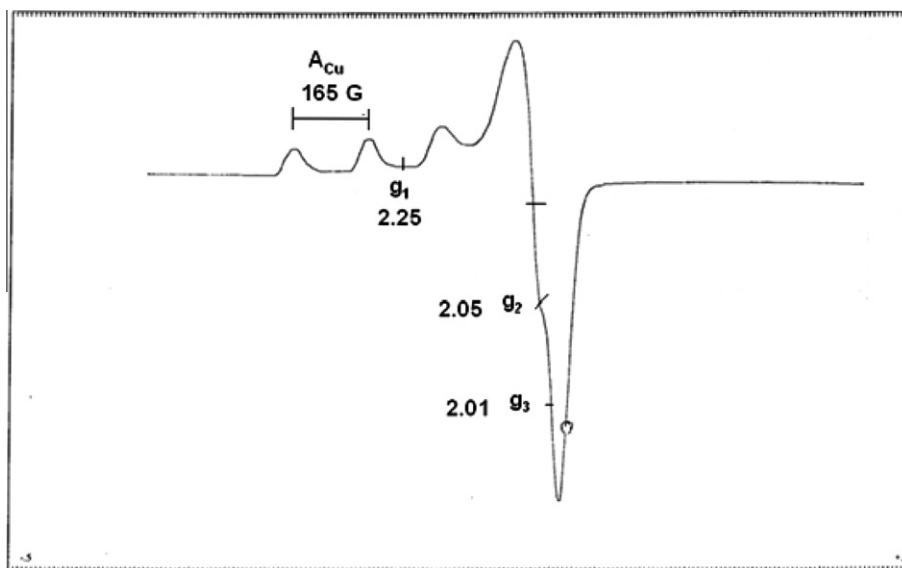


Fig. 2. X-band EPR spectrum of a frozen DMF solution of [Cu(HL)Cl] at liquid nitrogen temperature with TCNE as a standard.

Table 2
EPR and IR data.

Complex	IR data (cm ⁻¹) ^a			EPR		
	ν (C=C)	ν (Ar-C-O-C)	ν (C-O)	g_1	g_2	g_3
[Cu(HL)Cl] (1)	1608	1258	1377	2.25	2.05	2.01
[Ni(HL)Cl] (2)	1598	1257	1377			
[Zn(HL)Cl] (3)	1608	1258	1377			
[Fe(HL)Cl ₂] (4)	1609	1255	1377			

^a As a nujol mulls.

described as distorted trigonal bipyramidal (dtbp) with O₂, N₂ and O₃ forming the trigonal plane, and N₁ and Cl₁ occupying axial positions, with a predominant deviation in the trigonal plane as well as at the axial sites. The Cu–O₃ bond length is the shortest bond length followed by Cu–N₂, resulting in widening of the bond angle O₃–Cu–N₂, viz. 145.03°, and a contraction of the O₃–Cu–O₂ and N₂–Cu–O₂ angles from the ideal angle of 120°. A comparison of the bond angles in the trigonal plane formed by the pyridine nitrogen N₂, the hydroxylic oxygen O₂ and phenoxide the ion O₃ (108.07°, 145.03° and 104°) shows deviation from the ideal angle of 120° for a perfect trigonal plane, as well as that of the axial atoms N₁ and Cl₁ (average angles 84.36° and 95.02°) from 90°. An important feature of the structure is that the copper atom is shifted by about 0.172 Å from the N₂–O₂–O₃ plane towards Cl₁ atom (Supplementary Fig. S7).

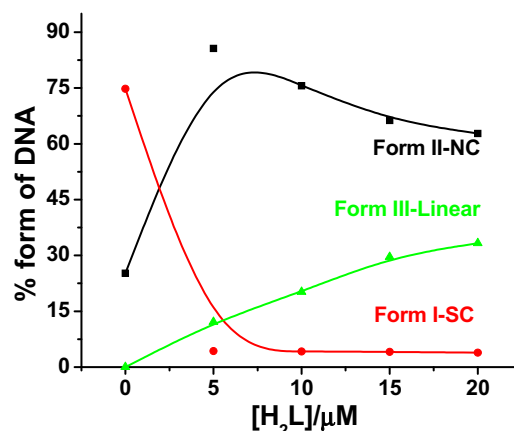


Fig. 3B. Concentration-dependent cleavage of pBR322 supercoiled plasmid DNA using 5, 10, 15 and 20 μM concentrations of H₂L.

A distorted sp arrangement can be visualized as N₁, N₂, Cl₁ and O₃ form an approximate square plane and O₂ occupies an axial position. Although the expected bond angle formed by the axial O₂ atom with any other donor atom is 90° at the copper center, it is observed to vary in the range 80.71–108.09°, suggesting a lot of distortion from an ideal sp arrangement.

The deviation from a perfect tbp as well as sp structure may be due to the difference in the electronegativities of all the different

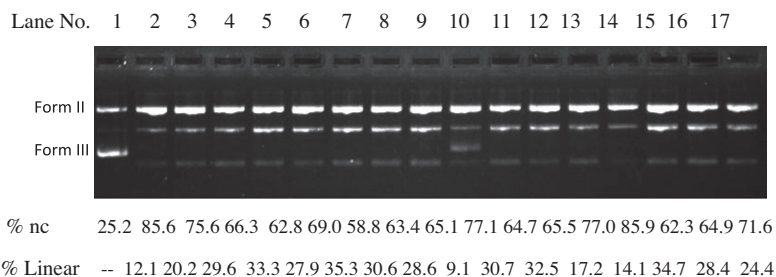


Fig. 3A. Agarose gel electrophoresis of pBR 322 DNA treated with increasing concentrations of ligand (H₂L) and its Cu (1), Ni (2) and Zn (3) complexes in TBE buffer (pH 8.2), [DNA] = 300 ng. Lane 1: DNA control; Lane 2: H₂L (5 μM) + DNA; Lane 3: H₂L (10 μM) + DNA; Lane 4: H₂L (15 μM) + DNA; Lane 5: H₂L (20 μM) + DNA; Lane 6: 1 (5 μM) + DNA; Lane 7: 1 (10 μM) + DNA; Lane 8: 1 (15 μM) + DNA; Lane 9: 1 (20 μM) + DNA; Lane 10: 2 (5 μM) + DNA; Lane 11: 2 (10 μM) + DNA; Lane 12: 2 (15 μM) + DNA; Lane 13: 2 (20 μM) + DNA; Lane 14: 3 (5 μM) + DNA; Lane 15: 3 (10 μM) + DNA; Lane 16: 3 (15 μM) + DNA; Lane 17: 3 (20 μM) + DNA.

Table 3

The K_b (binding constant) values for the ligand and the complexes.

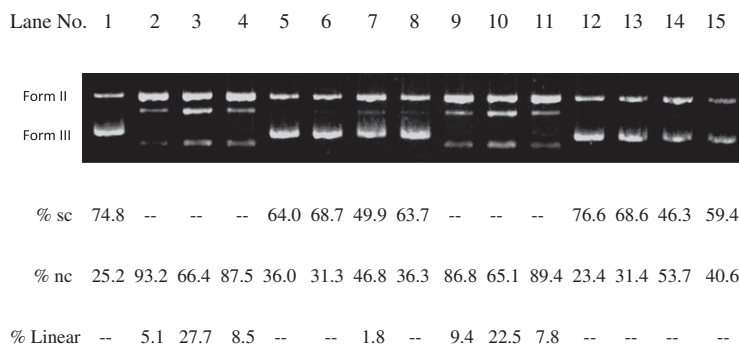
Ligand/complexes	K_b (M^{-1})
H₂L	5.33×10^5
[Cu(HL)Cl] (1)	6.47×10^3
[Ni(HL)Cl] (2)	4.56×10^4
[Zn(HL)Cl] (3)	6.70×10^3

coordinating atoms in the equatorial as well as axial sites, resulting in different bond lengths and bond angles (Table 1). A comparison of the bond lengths of the central metal-donor atoms shows that out of the two oxygen donors, the phenolic oxygen O3 is a stronger donor than the alkoxy oxygen O2 and amongst nitrogen donors, the pyridine nitrogen N2 is a stronger donor than the amine nitrogen N1. This has a net effect that the five bond lengths are all different, resulting in an intermediate structure between *tbp* and *sp*. Similarly, the adjacent five and six membered chelate rings might also be responsible for distortion from either of the ideal geometries. The τ parameter (equal to $\Delta/60^\circ$, where Δ is difference between the largest and next to largest ligand–metal–ligand angles) is useful geometrical discrimination, $\Delta = 60^\circ$, $\tau = 1$ for idealized *tbp* and $\Delta = 0$, $\tau = 0$ for idealized *sp*. The τ value of [Cu(HL)Cl] is 0.467, suggesting an almost intermediate structure between square pyramidal and trigonal bipyramidal [52].

4.2. Spectroscopy

The electronic spectra of all the complexes were recorded in DMF and in the solid state. From the identical UV–Vis spectra of the metal complexes in DMF and in the solid state, except for the nickel complex, it can be concluded that all the other complexes have the same structure, both in the solid state and in solution. The electronic spectra of the copper complex exhibits a ligand based transition λ_{max}/nm ($\epsilon/dm^3 mol^{-1} cm^{-1}$) around 284 (1860), a sharp peak at 460 (180) due to a ligand to metal charge transfer (LMCT) band and a well defined absorption at 704 (82) corresponding to a d–d transition assigned to a pentacoordinated copper(II) species having a stereochemistry distorted from regular square pyramidal or trigonal bipyramidal configurations. The iron complex shows ligand based bands at 275 (628), 302 (762) and 327 (1032), a charge transfer band at 340 (677) and a d–d transition absorption around 511 (504) due to Fe(III) in a distorted octahedral geometry [53]. The nickel complex shows absorptions at 280 (1920) and 302 (1910) and an absence of charge transfer and d–d transitions in DMF. While the solid state spectrum exhibits a charge transfer absorption at 390 nm and a d–d band at 629 nm, which clearly indicates that there is a difference in structure of the Ni complex in solution and in the solid state. Similarly, since the green complex on dissolution in DMF changes its color to almost colorless, coordination of the solvent to the vacant position is proposed. It is expected that Ni(II) would exhibit an absorption

(A)



(B)

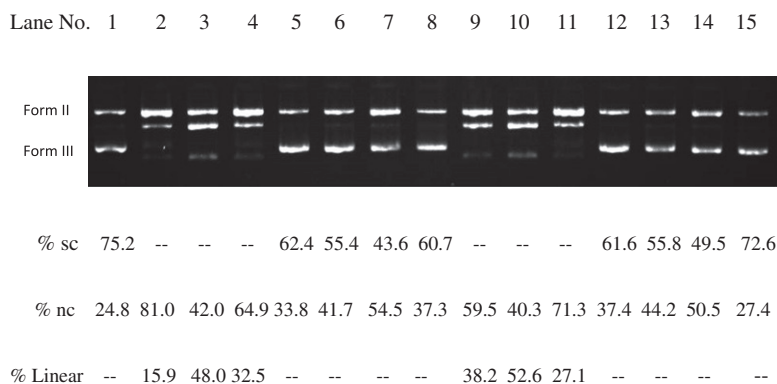


Fig. 4. Cleavage of pBR322 plasmid DNA (300 ng) by **H₂L** and **1** (20 μ M) in presence of radical scavengers. (A) Lane 1: DNA alone; Lane 2: DNA + **H₂L**; Lane 3: DNA + **H₂L** + DMSO (10 mM); Lane 4: DNA + **H₂L** + *D*-mannitol (50 mM); Lane 5: DNA + **H₂L** + DABCO (10 mM); Lane 6: DNA + **H₂L** + *L*-histidine (20 mM); Lane 7: DNA + **H₂L** + NaN₃ (20 mM); Lane 8: DNA + **H₂L** + SOD (15 units); Lane 9: DNA + **1**; Lane 10: DNA + **1** + DMSO (10 mM); Lane 11: DNA + **1** + *D*-mannitol (50 mM); Lane 12: DNA + **1** + DABCO (10 mM); Lane 13: DNA + **1** + *L*-histidine (20 mM); Lane 14: DNA + **1** + NaN₃ (20 mM); Lane 15: DNA + **1** + SOD (15 units); (B) **2** and **3** (20 μ M) in presence of radical scavengers. Lane 1: DNA alone; Lane 2: DNA + **2**; Lane 3: DNA + **2** + DMSO (10 mM); Lane 4: DNA + **2** + *D*-mannitol (50 mM); Lane 5: DNA + **2** + DABCO (10 mM); Lane 6: DNA + **2** + *L*-histidine (20 mM); Lane 7: DNA + **2** + NaN₃ (20 mM); Lane 8: DNA + **2** + SOD (15 units); Lane 9: DNA + **3**; Lane 10: DNA + **3** + DMSO (10 mM); Lane 11: DNA + **3** + *D*-mannitol (50 mM); Lane 12: DNA + **3** + DABCO (10 mM); Lane 13: DNA + **3** + *L*-histidine (20 mM); Lane 14: DNA + **3** + NaN₃ (20 mM); Lane 15: DNA + **3** + SOD (15 units).

in the visible region of electronic spectrum due to the presence of d electrons (d^8). However, we could not locate a d–d absorption for the complex when studied in DMF as a solvent, although we identified one in the solid state (at 15900 cm^{-1}). The absorption due to the d–d transition in the solid complex is weak. Therefore, it is suggested that due to the solvent effect (DMF, $\epsilon = 37$), the complex vibrations are suppressed or alternatively the complex may exist in a centrosymmetric octahedral form for which d–d transitions are forbidden on parity grounds [54,55]. The zinc complex exhibits only one ligand based transition at 288 (2100). The spectra of the iron and copper complexes have nearly the same transitions in both solid and solution states.

The frozen glass electron paramagnetic resonance spectrum of [Cu(HL)Cl] in DMF at liquid nitrogen temperature is shown in Fig. 2, while the EPR parameters and IR assignments are summarized in Table 2. The EPR spectrum of the copper complex shows four well resolved copper hyperfine lines, characteristic of a mononuclear copper(II) complex, and it exhibits three distinct features at 2.25, 2.05 and 2.01, corresponding to a distorted t_{bp}/sp structure with 165 G as the A_{Cu} component (shown in Fig. 2).

4.3. DNA cleavage

The DNA cleavage activity of the ligand, **H₂L** and its Cu(II) (**1**), Ni(II) (**2**) and Zn(II) (**3**) complexes has been studied using supercoiled plasmid pBR322 DNA in Tris–boric acid–EDTA (TBE) buffer in the absence of any external additives under dark conditions. The Fe(III) complex (complex **4**) was found to be very unstable in solution and hence was not studied. It was observed that all the compounds, including the ligand, convert supercoiled plasmid (SC) DNA into nicked circular (NC) DNA and the linear form (Figs. 3A and 3B) very efficiently, even at very low concentrations (10 μM). In addition, a low molecular weight band just below the supercoiled band is observed in all compounds. Further, the pattern of the DNA cleavage in all the complexes is similar to that of the ligand, which indicates a major role of the ligand in the DNA cleavage mechanism. Comparatively, more DNA cleavage is observed in **H₂L** and **3** followed by **2** and **1**.

To elucidate the mechanism involved in the DNA cleavage by these compounds, gel electrophoresis experiments were carried out in the presence of inhibitors of various reactive oxygen species like DMSO and mannitol ($\cdot\text{OH}$ radical inhibitor), DABCO (1,4-diazabicyclo [2.2.2] octane), NaN_3 and L-histidine (O_2 scavenger) and SOD (O_2^- scavenger). When singlet oxygen quenchers such as DABCO, sodium azide and L-histidine were added to the reaction mixture containing **H₂L**, **1**, **2** and **3**, inhibition of DNA cleavage activity was noted. These observations showed the involvement of singlet oxygen in the DNA cleavage reactions. Further, SOD activities showed $\sim 80\%$ inhibition of cleavage, indicating that superoxide radicals are also responsible for the DNA cleavage and the cleavage mechanism is oxidative (Fig. 4A and B).

4.4. DNA binding

The binding studies show hypochromism with an increase in the DNA concentration of CT-DNA. From the plot of $1/\Delta\epsilon_{ap}$ versus D , from Eq. (1), the intrinsic binding constant K_b was calculated and found to vary from 6.47×10^3 to $5.33 \times 10^5\text{ M}^{-1}$ and it is tabulated in Table 3. As can be seen from the table, the intrinsic binding constant of the ligand ($5.33 \times 10^5\text{ M}^{-1}$) is 100 fold higher compared to the Cu(II) and Zn(II) complexes ($\sim 6 \times 10^3\text{ M}^{-1}$). Interestingly, the Ni(II) complex shows an intrinsic binding 10 times higher than the Cu(II) and Zn(II) complexes. The ligand binds more strongly to the CT-DNA, followed by the Ni(II) complex. These binding constant values (K_b) are in good agreement with the DNA cleavage activity of the compounds.

5. Conclusion

An asymmetric tetradentate ligand **H₂L** and four metal complexes with approximate trigonal bipyramidal geometry have been prepared. All the compounds are effective in promoting cleavage of plasmid DNA at a minimum concentration of 5 μM by an oxidative mechanism. A binding investigation with CT-DNA confirmed that the ligand and metal complexes bind to the DNA. There is a close correlation between the K_b and the DNA cleavage pattern of the ligand and the complexes.

Acknowledgements

The authors acknowledge the RFSMS Fellowship from the University Grant Commission, India and are thankful to Dr. K.K. Sharma and Prof. K. J. Patil, School of Chemical Sciences, North Maharashtra University, India and Dr. E. Suresh, Central Marine Research Institute, Bhavnagar, India for the valuable discussions.

Appendix A. Supplementary data

CCDC 785617 contains the supplementary crystallographic data for structure [Cu(HL)Cl] (**1**). These data can be obtained free of charge via <http://www.ccdc.cam.ac.uk/conts/retrieving.html>, or from the Cambridge Crystallographic Data Centre, 12 Union Road, Cambridge CB2 1EZ, UK; fax: (+44) 1223-336-033; or e-mail: deposit@ccdc.cam.ac.uk. Supplementary data associated with this article can be found, in the online version, at [doi:10.1016/j.poly.2011.06.032](https://doi.org/10.1016/j.poly.2011.06.032).

References

- [1] S.J. Lippard, J.M. Berg, Principles of Bioinorganic Chemistry, University Science Books, Mill Valley, CA, 1994.
- [2] I. Bertini, H.B. Gray, S.J. Lippard, Bioinorganic Chemistry, University Science Books, Mill Valley, CA, 1994.
- [3] A.M. Pyle, J.K. Barton, Prog. Inorg. Chem. 38 (1990) 413.
- [4] K.E. Erkkila, D.T. Odum, J.K. Barton, Chem. Rev. 99 (1999) 2777.
- [5] J.K. Barton, Science 233 (1986) 727.
- [6] B. Armitage, Chem. Rev. 98 (1998) 1171.
- [7] D.R. McMillin, K.M. McNett, Chem. Rev. 98 (1998) 1201.
- [8] C. Metcalfe, J.A. Thomas, Chem. Soc. Rev. 32 (2003) 215.
- [9] B. Meunier, Chem. Rev. 92 (1992) 1411.
- [10] G. Pratviel, J. Bernadou, B. Meunier, Adv. Inorg. Chem. 45 (1998) 251.
- [11] W.K. Pogozelski, T.D. Tullius, Chem. Rev. 98 (1998) 1089.
- [12] C.J. Burrows, J.G. Muller, Chem. Rev. 98 (1998) 1109.
- [13] O. Zelenko, J. Gallagher, D.S. Sigman, Angew. Chem., Int. Ed. Engl. 36 (1997) 2776.
- [14] D.S. Sigman, T.W. Bruice, A. Mazumder, C.L. Sutton, Acc. Chem. Res. 26 (1993) 98.
- [15] L.E. Marshall, D.R. Graham, K.A. Reich, D.S. Sigman, Biochemistry 20 (1981) 244.
- [16] D.S. Sigman, D.R. Graham, V. D'Aurora, A.M. Stern, J. Biol. Chem. 254 (1979) 12269.
- [17] S.J. Lippard, Biochemistry 42 (2003) 2664.
- [18] E.R. Jamieson, S.J. Lippard, Chem. Rev. 99 (1999) 2467.
- [19] E.L. Hegg, J.N. Burstyn, Coord. Chem. Rev. 173 (1998) 133.
- [20] J. Reedijk, J. Inorg. Biochem. 86 (2001) 89.
- [21] S.E. Wolkenberg, D.L. Boger, Chem. Rev. 102 (2002) 2477.
- [22] A. Sreedhara, J.A. Cowan, J. Biol. Inorg. Chem. 6 (2001) 337.
- [23] H. Ali, J.E. Van Lier, Chem. Rev. 99 (1999) 2379.
- [24] A.K. Patra, S. Dhar, M. Nethaji, A.R. Chakravarty, J. Chem. Soc., Dalton Trans. 5 (2005) 896.
- [25] M. Roy, R. Santhanagopal, A.R. Chakravarty, J. Chem. Soc., Dalton Trans. (2009) 1024.
- [26] B. Lippert, Coord. Chem. Rev. 200–202 (2000) 487.
- [27] D.S. Sigman, A. Mazumder, D.M. Perrin, Chem. Rev. 93 (1993) 2295.
- [28] P.B. Dervan, Science 232 (1986) 464.
- [29] D.S. Sigman, T.W. Bruice, A. Mazumder, C.L. Sutton, Acc. Chem. Res. 26 (1992) 98.
- [30] J. Stubbe, J.W. Kozarich, Chem. Rev. 87 (1987) 1107.
- [31] J.C. Babrowaik, B. Ward, G. Goodisman, Biochemistry 28 (1989) 3314.
- [32] C.J. Burrows, S.E. Rokita, Acc. Chem. Res. 27 (1994) 295.
- [33] D.J. Gravert, J.H. Griffin, Inorg. Chem. 35 (1995) 4837.
- [34] R.R. Joshi, S.M. Likhite, R.K. Kumar, K.N. Ganesh, Biochim. Biophys. Acta 1199 (1994) 285.

- [35] V.W.-W. Yam, S.W.-K. Choi, K.K.-W. Lo, W.-F. Dung, R.V.-C. Kong, *J. Chem. Soc., Chem. Commun.* (1994) 2379.
- [36] A.S. Sitali, E.C. Long, A.M. Pyle, J.K. Barton, *J. Am. Chem. Soc.* 114 (1992) 2303.
- [37] E. Lamour, S. Routier, J.L. Bernier, J.P. Catteau, C. Bailly, H. Vezin, *J. Am. Chem. Soc.* 121 (1999) 1862.
- [38] C. Sissi, F. Mancin, M. Gatos, M. Palumbo, P. Tecilla, U. Tonellato, *Inorg. Chem.* 44 (2005) 2310.
- [39] S.S. Tonde, A.S. Kumbhar, S.B. Pdhye, R.J. Butcher, *J. Inorg. Biochem.* 100 (2006) 51.
- [39] B.N. Trawick, A.T. Daniher, J.K. Bashkin, *Chem. Rev.* 98 (1998) 939.
- [41] S.J. Behroozi, W. Kim, J. Dannaldson, K.S. Gates, *Biochemistry* 35 (1996) 1768.
- [42] K. Mitra, W. Kim, J.S. Daniels, K.S. Gates, *J. Am. Chem. Soc.* 119 (1997) 11691.
- [43] A. Neves, M.A. de Brito, V. Drago, K. Griesar, W. Haase, *Inorg. Chim. Acta* 237 (1995) 131.
- [44] G.M. Sheldrick, SAINT and XPREP, Version 5.1, Siemens Industrial Automation Inc., Madison, WI, 1995.
- [45] SADABS Empirical Absorption Correction Program, University of Gottingen, Germany, 1997.
- [46] G.M. Sheldrick, SHELXTL V5.1 Software Reference Manual, Bruker AXS, Inc., Madison, WI, USA, 1997.
- [47] G.M. Sheldrick, SHELXL-97, A Program for Refining Crystal Structures, University of Gottingen, Germany, 1997.
- [48] C.K. Johnson, ORTEP. Report ORNL-5138, Oak Ridge National Laboratory, TN, USA, 1976.
- [49] A.L. Spek, PLATON, A Multipurpose Crystallographic Tool, Utrecht University, Utrecht, The Netherlands, 1999.
- [50] A. Wolfe, G.H. Shimer Jr., T. Meehan, *Biochemistry* 26 (20) (1987) 6392.
- [51] D.E.V. Schmechel, D.M. Crothers, *Biopolymers* 10 (1971) 465.
- [52] B. Baruah, S.P. Rath, A. Chakravorty, *Eur. J. Chem.* (2004) 1873.
- [53] A.B.P. Lever, *Inorganic Electronic Spectroscopy*, second ed., Elsevier.
- [54] R.S. Drago, *Physical Methods in Chemistry*, Saunders Golden Sunburst Series, (1977) 382.
- [55] P.W. Atkins, *Physical Chemistry*, third ed., Oxford University Press, p.468.



Mrs Anupa A. Kumbhar, Assistant Professor, Department of Chemistry, University of Pune, Pune 411007, India.



Mrs R. S. Bendre, Associate Professor, School of Chemical Sciences, North Maharashtra University, Jalgaon 425001, India.



Mr. Rakesh S. Sancheti, Research Fellow, School of Chemical Sciences, North Maharashtra University, Jalgaon 425001, India.